

Synthesis and Reactivity of a Diruthenium Diazoalkane Complex

Yuan Gao, Michael C. Jennings, and Richard J. Puddephatt*

Department of Chemistry, University of Western Ontario, London, Ontario, Canada N6A 5B7

Hilary A. Jenkins

Department of Chemistry, St. Mary's University, Halifax, Nova Scotia, Canada B3H 3C

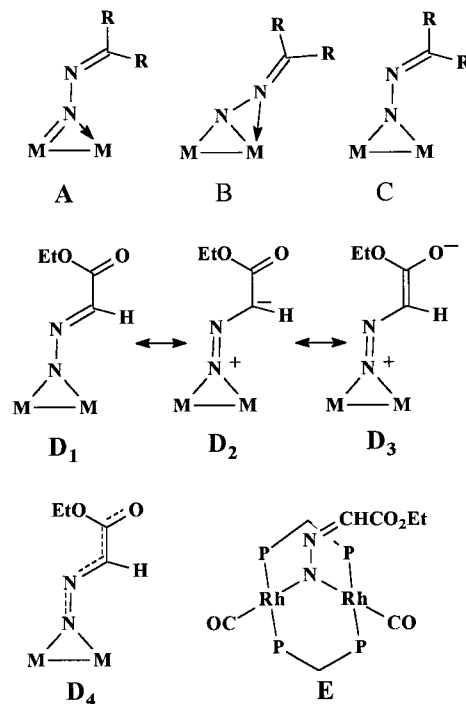
Received March 22, 2001

Reaction of $[\text{Ru}_2(\mu\text{-CO})(\text{CO})_4(\mu\text{-dppm})_2]$, **1**, $\text{dppm} = \text{Ph}_2\text{PCH}_2\text{PPh}_2$, with $\text{N}_2\text{CHCO}_2\text{Et}$ gives the complex $[\text{Ru}_2(\mu\text{-NNCHCO}_2\text{Et})(\text{CO})_4(\mu\text{-dppm})_2]$, **2**, in which the diazoalkane acts as a novel 2-electron ligand bridging a metal–metal bond. Complex **2** reacts with phenylacetylene, with displacement of a carbonyl ligand, to give $[\text{Ru}_2(\mu\text{-CO})(\text{CO})_2\{\mu\text{-NN}(\text{CHCO}_2\text{Et})(\text{CPh}=\text{CH})\}(\mu\text{-dppm})_2]$, **3a**, which contains a new type of metallacycle formed by coupling of the diazoalkane and alkyne ligands at the diruthenium center. Protons attack complex **2** first at the NCH center to give the alkyldiazonium complex $[\text{Ru}_2(\text{CO})_4(\mu\text{-NNCH}_2\text{CO}_2\text{Et})(\mu\text{-dppm})_2]^+$, **4**, and then, with the strong acid $\text{H}[\text{BF}_4]$, at the Ru–Ru bond to give the dicationic complex $[\text{Ru}_2(\mu\text{-H})(\text{CO})_4(\mu\text{-NNCH}_2\text{CO}_2\text{Et})(\mu\text{-dppm})_2]^{2+}$, **5**. Complex **2** is a precatalyst for the decomposition of formic acid to give CO_2 and H_2 , and the chemistry leading to the active catalyst is described.

Introduction

Transition-metal diazoalkane complexes are of interest as intermediates in the formation of alkyldiene complexes and in catalytic transfer of alkyldiene groups,¹ but also because they can exhibit several unusual coordination modes² and may model intermediates in the fixation of dinitrogen to give organonitrogen compounds.³ There are still relatively few complexes in which a diazoalkane bridges between two metal atoms, and most of these are with early transition metals. In these complexes, the diazoalkane usually acts as a 4-electron ligand, with structure **A** or **B** (Chart 1).² There appear to be no structurally characterized examples of binuclear complexes with 2-electron bridging diazoalkane ligands of type **C** (Chart 1). In the case with diazoalkane = ethyl diazoacetate, there are several resonance forms possible for a 2-electron donor (e.g., **D**₁–**D**₃ in Chart 1) and extended π -conjugation is possible as shown in **D**₄ (Chart 1, participation by metal $d(\pi)$ orbitals is also likely but is not shown).² The binuclear rhodium complex $[\text{Rh}_2(\text{CO})_2(\mu\text{-dppm})_2(\mu\text{-N}_2\text{-CHCO}_2\text{Et})]$, $\text{dppm} = \text{Ph}_2\text{PCH}_2\text{PPh}_2$, (Chart 1, **E**) may be of this bonding type, based on its spectroscopic data, but it does not contain a metal–metal bond.⁴

Chart 1



(1) (a) Sutton, D. *Chem. Rev.* **1993**, *93*, 995. (b) Doyle, M. P. *Chem. Rev.* **1986**, *86*, 919. (c) Herrmann, W. A. *Angew. Chem., Int. Ed. Engl.* **1978**, *17*, 800. (d) Hillhouse, G. L.; Haymore, B. L. *J. Am. Chem. Soc.* **1982**, *104*, 1537. (e) Galardon, E.; Le Maux, P.; Simonneaux, G. *Tetrahedron* **2000**, *56*, 615. (f) Baratta, W.; Herrmann, W. A.; Kratzer, R. M.; Rigo, P. *Organometallics* **2000**, *19*, 3664. (g) Noels, A. F.; Demonceau, A. *J. Phys. Org. Chem.* **1998**, *11*, 602. (h) Nishiyama, H.; Itoh, Y.; Matsumoto, H.; Park, S. B.; Itoh, K. *J. Am. Chem. Soc.* **1994**, *116*, 2223.

(2) (a) Mizobe, Y.; Ishii, Y.; Hidai, M. *Coord. Chem. Rev.* **1995**, *139*, 281. (b) Dartiguenave, M.; Menu, M. J.; Deydier, E.; Dartiguenave, Y.; Siebald, H. *Coord. Chem. Rev.* **1998**, *178–180*, 623.

(3) (a) Hidai, M.; Mizobe, Y. *Chem. Rev.* **1995**, *95*, 1115. (b) Harada, Y.; Mizobe, Y.; Ishii, Y.; Hidai, M. *Bull. Chem. Soc. Jpn.* **1998**, *71*, 2701.

(4) Woodcock, C.; Eisenberg, R. *Organometallics* **1985**, *4*, 4.

This paper reports the first example of a diruthenium μ -diazoalkane complex, establishes that the diazoalkane serves as a 2-electron ligand, and describes a study of the reactivity of this compound. It has previously been shown that a diruthenium μ -methylene complex, $[\text{Ru}_2(\mu\text{-CH}_2)(\text{CO})_4(\mu\text{-dppm})_2]$, is formed by reaction of CH_2N_2 with $[\text{Ru}_2(\mu\text{-CO})(\text{CO})_4(\mu\text{-dppm})_2]$, **1**.⁵

(5) Gao, Y.; Jennings, M. C.; Puddephatt, R. J. *Organometallics* **2001**, *20*, 1882.

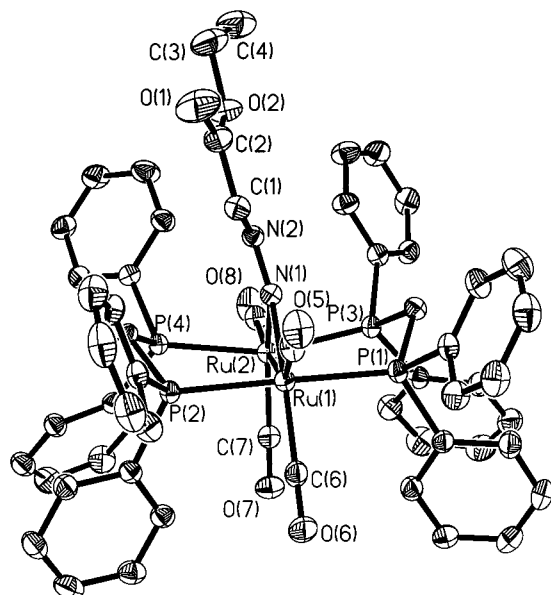
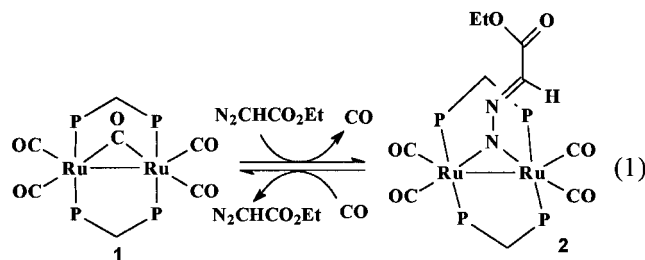


Figure 1. A view of the structure of complex **2**. Thermal ellipsoids are shown at the 25% probability level.

Results and Discussion

Synthesis and Characterization of $[\text{Ru}_2(\mu\text{-}\eta^1\text{-}\eta^1\text{-NNCHCO}_2\text{Et})(\text{CO})_4(\mu\text{-dppm})_2]$, **2.** The reaction of ethyl diazoacetate with complex **1** occurred according to eq 1 to give the product $[\text{Ru}_2\{\mu\text{-NNCHCO}_2\text{Et}\}(\text{CO})_4(\mu\text{-dppm})_2]$, **2**, as a brown-red, air-stable solid that was isolated in 56% yield. The reaction of eq 1 is reversible,



and reaction of **2** with excess CO gave back complex **1**. Complex **2** appears to be the first example of a diruthenium diazoalkane complex, and it was characterized by its spectroscopic properties and by an X-ray structure determination.

The molecular structure of **2** is shown in Figure 1, and selected bond lengths and angles are listed in Table 1. As shown in Figure 1, the complex contains a *trans,trans*- $\text{Ru}_2(\mu\text{-dppm})_2$ unit, with four terminal carbonyl ligands and a bridging ethyl diazoacetate ligand. The distance $\text{Ru}-\text{Ru} = 2.8550(4)$ Å is typical for a single $\text{Ru}-\text{Ru}$ bond⁶⁻⁹ and similar to that found in complex **1** ($\text{Ru}-\text{Ru} = 2.903(2)$ Å in the acetone solvate).⁶ Therefore, the reaction of eq 1 occurs by simple displacement of $\mu\text{-CO}$ by $\mu\text{-NNCHCO}_2\text{Et}$, and on the basis of the 18-

Table 1. Selected Bond Distances and Angles in **2**

Bond Distances (Å)			
$\text{Ru}(1)-\text{Ru}(2)$	2.8550(4)	$\text{Ru}(1)-\text{P}(1)$	2.3507(9)
$\text{Ru}(1)-\text{P}(2)$	2.3472(9)	$\text{Ru}(2)-\text{P}(3)$	2.3621(10)
$\text{Ru}(2)-\text{P}(4)$	2.3671(9)	$\text{Ru}(1)-\text{C}(5)$	1.908(4)
$\text{Ru}(1)-\text{C}(6)$	1.914(4)	$\text{Ru}(2)-\text{C}(7)$	1.895(4)
$\text{Ru}(2)-\text{C}(8)$	1.889(4)	$\text{Ru}(1)-\text{N}(1)$	2.094(3)
$\text{Ru}(2)-\text{N}(1)$	2.075(3)	$\text{N}(1)-\text{N}(2)$	1.270(4)
$\text{N}(2)-\text{C}(1)$	1.328(5)	$\text{C}(1)-\text{C}(2)$	1.433(6)
$\text{C}(2)-\text{O}(1)$	1.201(5)	$\text{C}(2)-\text{O}(2)$	1.365(5)
$\text{C}(3)-\text{O}(2)$	1.440(6)	$\text{C}(3)-\text{C}(4)$	1.549(9)
$\text{C}(5)-\text{O}(5)$	1.137(5)	$\text{C}(6)-\text{O}(6)$	1.136(5)
$\text{C}(7)-\text{O}(7)$	1.145(5)	$\text{C}(8)-\text{O}(8)$	1.129(5)

Bond Angles (deg)			
$\text{P}(1)-\text{Ru}(1)-\text{P}(2)$	178.47(3)	$\text{P}(3)-\text{Ru}(2)-\text{P}(4)$	161.92(4)
$\text{P}(1)-\text{Ru}(1)-\text{N}(1)$	90.13(8)	$\text{P}(2)-\text{Ru}(1)-\text{N}(1)$	90.06(3)
$\text{P}(3)-\text{Ru}(2)-\text{N}(1)$	86.03(8)	$\text{P}(4)-\text{Ru}(2)-\text{N}(1)$	85.58(8)
$\text{Ru}(1)-\text{N}(1)-\text{Ru}(2)$	46.50(8)	$\text{C}(1)-\text{N}(2)-\text{N}(1)$	124.6(3)
$\text{C}(2)-\text{C}(1)-\text{N}(2)$	119.74(3)	$\text{C}(5)-\text{Ru}(1)-\text{N}(1)$	101.22(15)
$\text{C}(6)-\text{Ru}(1)-\text{N}(1)$	162.51(16)	$\text{C}(7)-\text{Ru}(2)-\text{N}(1)$	140.24(14)
$\text{C}(8)-\text{Ru}(2)-\text{N}(1)$	120.15(16)		

electron rule, the $\mu\text{-NNCHCO}_2\text{Et}$ ligand is expected to act as a 2-electron ligand in complex **2**.

The ethyl diazoacetate ligand is very roughly planar (the twist away from planarity is clear in Figure 1), and it is also roughly coplanar with the $\text{Ru}_2(\text{CO})_4$ atoms. The distances $\text{Ru}(1)-\text{N}(1) = 2.094(3)$ Å and $\text{Ru}(2)-\text{N}(1) = 2.075(3)$ Å suggest single bonds and appear inconsistent with bonding mode **A** (Chart 1), for which the $\text{M}=\text{N}$ bond is expected to be short.^{2,10} The ethyl diazoacetate is bent at $\text{N}(2)$ with the angle $\text{C}(1)-\text{N}(2)-\text{N}(1) = 124.6(3)^\circ$, suggesting sp^2 hybridization at $\text{N}(2)$, but $\text{N}(2)$ is clearly not coordinated to ruthenium and the bonding mode **B** of Chart 1 is ruled out. The distances $\text{N}(1)-\text{N}(2) = 1.270(4)$ Å, $\text{C}(1)-\text{N}(2) = 1.328(5)$ Å, and $\text{C}(1)-\text{C}(2) = 1.433(6)$ Å and $\text{C}(2)-\text{O}(1) = 1.201(5)$ Å are all shorter than expected for single bonds. Together with the approximate planarity of these atoms, the pattern of bond distances supports the presence of NNCCO conjugation, with $\text{Ru}-\text{N}$ single bonds, as depicted in **D**₄ (Chart 1). The representation as **2** in eq 1 is clearly oversimplified, since it represents only one canonical form (**D**₁ in Chart 1).

The $\text{Ru}_2\text{P}_2\text{C}_2$ atoms of the $\text{Ru}_2(\mu\text{-dppm})_2$ unit are in the extended boat conformation with the two methylene carbon atoms directed above the Ru_2P_4 plane, toward the diazoalkane ligand. The conformation is probably determined by the need to minimize steric effects between the phenyl substituents of the dppm ligands and the carbonyl and diazoalkane ligands (Figure 1). The distortion of PRuP angles from linearity is much greater at $\text{Ru}(2)$ [$\text{P}(3)-\text{Ru}(2)-\text{P}(4) = 161.92(4)^\circ$] than at $\text{Ru}(1)$ [$\text{P}(1)-\text{Ru}(1)-\text{P}(2) = 178.47(3)^\circ$]. It is also noteworthy that the $\text{Ru}-\text{P}$ bonds are longer but the $\text{Ru}-\text{C}$ bonds and $\text{Ru}-\text{N}$ bond are slightly shorter at $\text{Ru}(2)$ compared to $\text{Ru}(1)$ (Table 1), but it is not clear if these differences are caused by electronic or steric effects.

The spectroscopic data for **2** are consistent with the solid structure. The IR spectrum contains four peaks for the four terminal carbonyl ligands at $\nu(\text{CO}) = 1974$, 1955, 1929, and 1900 cm^{-1} . The ethyl diazoacetate ligand gave a peak at 1632 cm^{-1} for $\nu(\text{C}=\text{O})$ and a peak at 1574 cm^{-1} for $\nu(\text{C}=\text{N})$. The stretching frequency for

(6) Kuncheria, J.; Mirza, H. A.; Jenkins, H. A.; Vittal, J. J.; Puddephatt, R. J. *J. Chem. Soc., Dalton Trans.* **1998**, 285.

(7) Mirza, H. A.; Vittal, J. J.; Puddephatt, R. J. *Inorg. Chem.* **1993**, *32*, 1327.

(8) Engel, D. W.; Moodley, K. G.; Subramony, L.; Haines, R. J. *J. Organomet. Chem.* **1988**, *349*, 393. Ferrence, G. M.; Fanwick, P. E.; Kubiak, C. P.; Haines, R. J. *Polyhedron* **1997**, *16*, 1453.

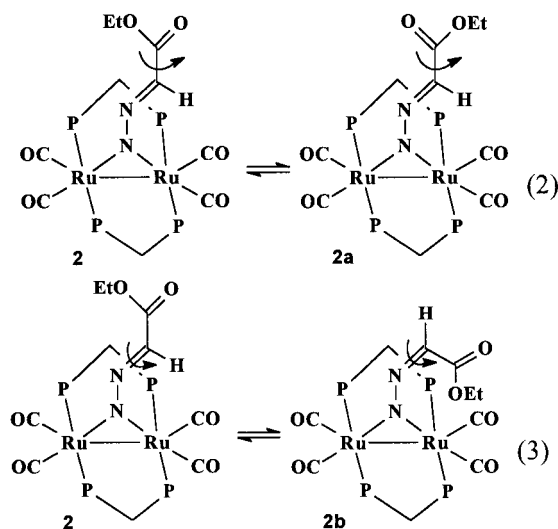
(9) Kuncheria, J.; Mirza, H. A.; Vittal, J. J.; Puddephatt, R. J. *J. Organomet. Chem.* **2000**, *593-594*, 77.

(10) Curtis, M. D.; Messerle, L.; D'Errico, J. J.; Butler, W. M.; Hay, M. S. *Organometallics* **1986**, *5*, 2283.

$\nu(\text{C}=\text{O}) = 1632 \text{ cm}^{-1}$ for the ethyl diazoacetate ligand of **2** is significantly lower than that in the free ligand, which has $\nu(\text{C}=\text{O}) = 1730 \text{ cm}^{-1}$. This difference is caused by the conjugation in **2**, with a contribution from the canonical form **D₃** in Chart 1, leading to a CO bond order less than two. A similar rationale was offered for the reduced value of $\nu(\text{C}=\text{O}) = 1610 \text{ cm}^{-1}$ in **E** (Chart 1).⁴

In solution, complex **2** was fluxional, as shown by variable temperature NMR studies. At room temperature, the spectra were broad but consistent with the expected C_s symmetry for complex **2**. Thus, the $^{31}\text{P}\{\text{H}\}$ NMR spectrum of **2** contained two multiplets at $\delta = 26.3$ and 33.0 , and the ^1H NMR spectrum contained a singlet at $\delta = 5.8$ (NCH) and multiplets at $\delta = 4.3$ (CH_2) and 1.5 (CH_3) for the ethyl diazoacetate ligand and two partly overlapped multiplets centered at $\delta = 3.1$ for the CH_2 protons of the dppm ligands. The $^{13}\text{C}\{\text{H}\}$ NMR spectrum of a ^{13}CO -labeled sample of **2** showed four resonances at $\delta = 198, 198.4, 210,$ and 214.8 for the four carbonyl ligands.

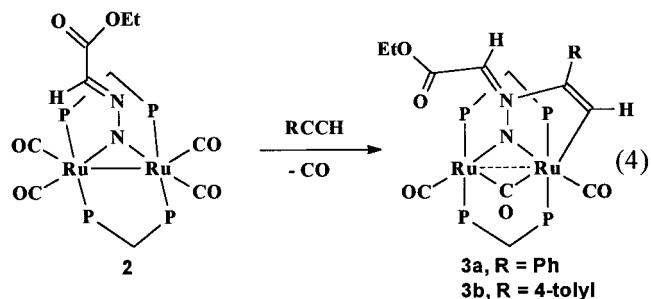
On reducing the temperature to about -10°C , each peak observed in the room temperature NMR spectrum had split into two, with relative intensities of ca. 3:2. For example, the NCH proton appeared as two broad singlets at $\delta = 5.8$ and 5.65 in the ^1H NMR spectrum and the dppm phosphorus atoms gave two sets of resonances at $\delta = 25.8$ and 32.0 and at $\delta = 26.0$ and 33.0 in the $^{31}\text{P}\{\text{H}\}$ NMR spectrum. No further splitting occurred on cooling to -90°C . These data clearly indicate that complex **2** exists in solution as a 3:2 mixture of two rapidly equilibrating isomeric forms, each having C_s symmetry. The isomers probably occur as a result of restricted rotation about the C(1)–C(2) bond as shown in eq 2. The data do not exclude rotation



about the N(2)–C(1) bond (eq 3), but this is considered improbable both because there is more double bond character and because a bigger difference in chemical shifts of the two isomers would be expected. A similar isomerization was observed in dimolybdenum complexes, in which the diazoalkane is present as a 4-electron ligand.¹⁰

Reactions of Complex 2 with Alkynes: Syntheses of Complexes $[\text{Ru}_2(\mu\text{-CO})(\text{CO})_2\{\mu\text{-EtOC(O)C(H)N(N)C(R)=CH}\}(\mu\text{-dppm})_2]$, **3a, **R = Ph**; **3b**, **R =****

4-Tolyl. The reaction of excess $\text{PhC}\equiv\text{CH}$ with complex **2** in a dichloromethane solution for 3 h gave the complex $[\text{Ru}_2(\mu\text{-CO})(\text{CO})_2\{\mu\text{-NN}(\text{CHCO}_2\text{Et})(\text{CPh}=\text{CH})\}(\mu\text{-dppm})_2]$, **3a**, according to eq 4. When monitored by



NMR, **3a** was shown to be formed almost quantitatively, and it was isolated as an air-stable, brown-yellow solid in 60% yield. Complex **3b** was synthesized in a similar manner, but complex **2** did not react with the alkynes PhCCPh , PhCCMe , EtCCEt , or $n\text{-BuCCH}$. Complex **2** reacted rapidly with the alkynes HCCCO_2Me and $\text{MeO}_2\text{CCCCO}_2\text{Me}$, but complex mixtures of products were formed. The solid-state structures of **3a** and **3b** were established by X-ray diffraction studies, as well as by spectroscopic methods.

The molecular structures of **3a** and **3b** are shown in Figure 2, and selected bond lengths and bond angles are listed in Table 2. The complexes **3a** and **3b** are isomorphous and isostructural. The structure solutions were difficult due to disorder as described below. The second structure determination was carried out in the frustrated hope of a simpler solution. Since **3b** gave better data, only its structure is discussed. The complexes contain a crystallographic 2-fold axis that passes through the atoms N(1)N(2)C(16)O(16); the atoms of the ligand arising from combination of the diazoalkane and alkyne ligands, except N(1) and N(2), are disordered 50:50 by the C_2 operation. Only one component is shown for each of **3a** and **3b** in Figure 2, but it should be clear that several atoms in the disorder model will appear to be very close together and were difficult to resolve. A reasonable solution was obtained in each case, but the atoms of the ethoxy group were poorly defined and it is likely that there is additional disorder of these atoms.

As shown in Figure 2, complex **3b** contains a *trans,trans*- $\text{Ru}_2(\mu\text{-dppm})_2$ unit, in a boat conformation similar to that in **2**. Each ruthenium in **3b** has one terminal carbonyl ligand and there is one bridging carbonyl. The remaining ligand is formed by combination of the ethyl diazoacetate and 4-tolyl acetylene groups, with N(1) bridging the two ruthenium atoms and C(1) terminally bound to one of the ruthenium atoms. The five-membered ring $\text{RuN}(1)\text{N}(2)\text{C}(2)\text{C}(1)$ can be considered to be formed by regioselective (3 + 2)-cycloaddition of the alkyne across the $\text{RuN}(1)\text{N}(2)$ unit in **2**, though with a change in stereochemistry about the $\text{N}=\text{C}$ bond (eq 4). The distance $\text{Ru}-\text{RuA} = 3.117(1) \text{ \AA}$ is longer than expected for a typical $\text{Ru}-\text{Ru}$ single bond ($2.71\text{--}3.02 \text{ \AA}$),^{6–9} but short enough that a weak bond cannot be discounted. The carbonyl oxygen atom O(2) lies close to RuA but the distance $\text{RuA}-\text{O}(2) = 2.60 \text{ \AA}$ is too long to represent a covalent bond, and the pattern of bond angles within the diazoalkane fragment [e.g., $\text{N}(1)\text{N}(2)\text{C}(11) = 143.0(8)^\circ$] indicates that the $\text{RuA}\cdots\text{O}(2)$

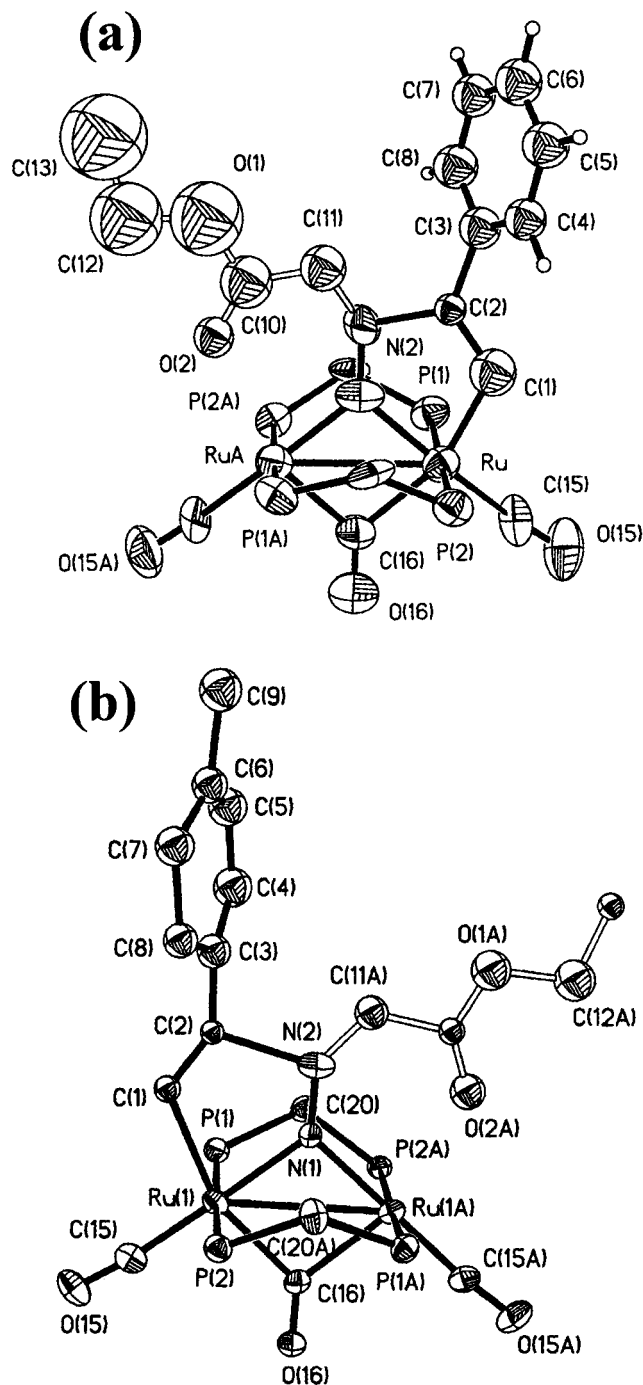


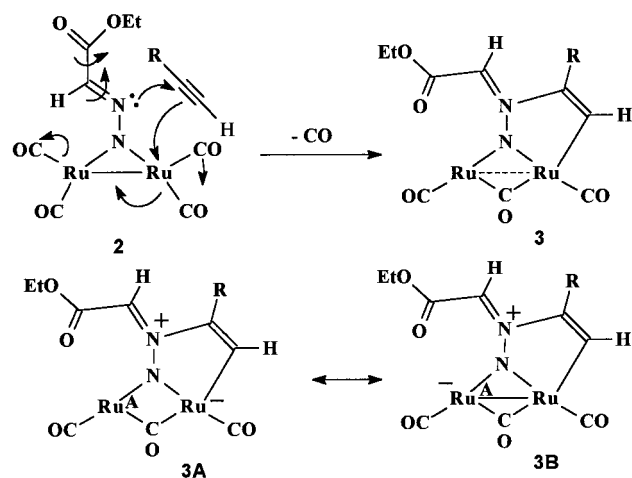
Figure 2. Views of the structures of (a) complex **3a** and (b) complex **3b**. The organic ligand is disordered by a C_2 axis passing through N(1)N(2), and Figures 2a and 2b roughly represent the two components of the disorder model.

interaction may be repulsive.¹¹ The atoms O(2)C(10)C(11)N(2)N(1)C(2)C(1) are roughly coplanar with the $Ru_2(CO)_2(\mu-CO)$ unit, indicative of π -conjugation in the complex ligand. The stereochemistry about the N(2)=C(11) bond is opposite from that in the parent complex **2** (similar to **2b** in eq 3), but most distances within the diazoacetate fragment are similar in **2** and **3b**. The bond

Table 2. Selected Bond Distances and Angles in **3a**·1/2CH₂Cl₂ and **3b**

	3a	3b
Bond Distances (Å)		
Ru–RuA	3.108(3)	3.117(1)
Ru–P(1)	2.344(5)	2.340(2)
Ru–P(2)	2.353(4)	2.353(2)
Ru–C(15)	1.85(2)	1.836(1)
Ru–C(16)	2.07(2)	2.093(6)
Ru–C(1)	1.99(5)	2.24(2)
Ru–N(1)	2.02(1)	2.061(5)
N(1)–N(2)	1.33(2)	1.26(1)
N(2)–C(2)	1.63(5)	1.63(2)
N(2)–C(11)	1.30(4)	1.30(2)
C(1)–C(2)	1.44(6)	1.40(3)
C(10)–C(11)	1.45(7)	1.38(3)
C(10)–O(2)	1.21(5)	1.20(2)
C(10)–O(1)	1.42(6)	1.44(2)
C(12)–O(1)	1.49(1)	1.54(3)
C(12)–C(13)	1.49(5)	1.54(1)
C(15)–O(15)	1.13(2)	1.143(8)
C(16)–O(16)	1.21(3)	1.19(1)
Bond Angles (deg)		
P(1)–Ru–P(2)	173.8(2)	173.92(7)
P(1)–Ru–N(1)	86.4(1)	86.39(5)
P(2)–Ru–N(1)	89.3(1)	89.12(5)
P(1)–Ru–RuA	89.8(1)	89.59(5)
P(2)–Ru–RuA	89.7(1)	89.71(5)
P(1)–Ru–N(1)	86.4(1)	86.39(5)
P(2)–Ru–N(1)	89.3(1)	89.12(5)
Ru–N(1)–RuA	100(1)	98.2(3)
C(2)–N(2)–N(1)	102(2)	104.3(8)
C(11)–N(2)–N(1)	145(2)	143.0(8)
Ru–N(1)–N(2)	129.9(5)	130.9(1)
Ru–C(1)–C(2)	118(4)	109(1)
C(1)–Ru–N(1)	76.2(15)	75.3(5)
N(2)–C(11)–C(10)	110(4)	108(2)
C(1)–C(2)–N(2)	114(4)	119(2)
C(15)–Ru–N(1)	177.1(7)	177.1(3)
C(16)–Ru–N(1)	81.4(7)	82.8(2)

Scheme 1. dppm Ligands Are Omitted for Clarity



distance Ru–N(1) = 2.061(5) Å is slightly shorter than the Ru–N bonds in **2**, while Ru(1)–C(1) = 2.24(2) Å is in the range expected for a Ru–C single bond.¹²

In complex **3b**, ignoring any metal–metal bonding, the stereochemistry about Ru(1) and Ru(1A) is roughly octahedral and square pyramidal, respectively. Clearly

(11) (a) Gambarotta, S.; Floriani, C.; Chiesi-Villa, A.; Guastini, C. *J. Am. Chem. Soc.* **1982**, *104*, 1918. (b) Johnson, K. A.; Vashon, M. D.; Moasser, B.; Warmka, B. K.; Gladfelter, W. L. *Organometallics* **1995**, *14*, 461. (c) Herrero, P. G.; Weberndorfer, B.; Ilg, K.; Wolf, J.; Werner, H. *Angew. Chem., Int. Ed.* **2000**, *39*, 3267.

(12) It is likely that at least some of the atoms N(2)N(1)C(16)O(16) lie slightly off of the 2-fold axis, but the displacements were not large enough to allow resolution of the resulting disorder. Extensive discussion of bond parameters involving disordered atoms is not justified. The distance C(2A)–N(2) = 1.63(2) appears anomalously long, for example.

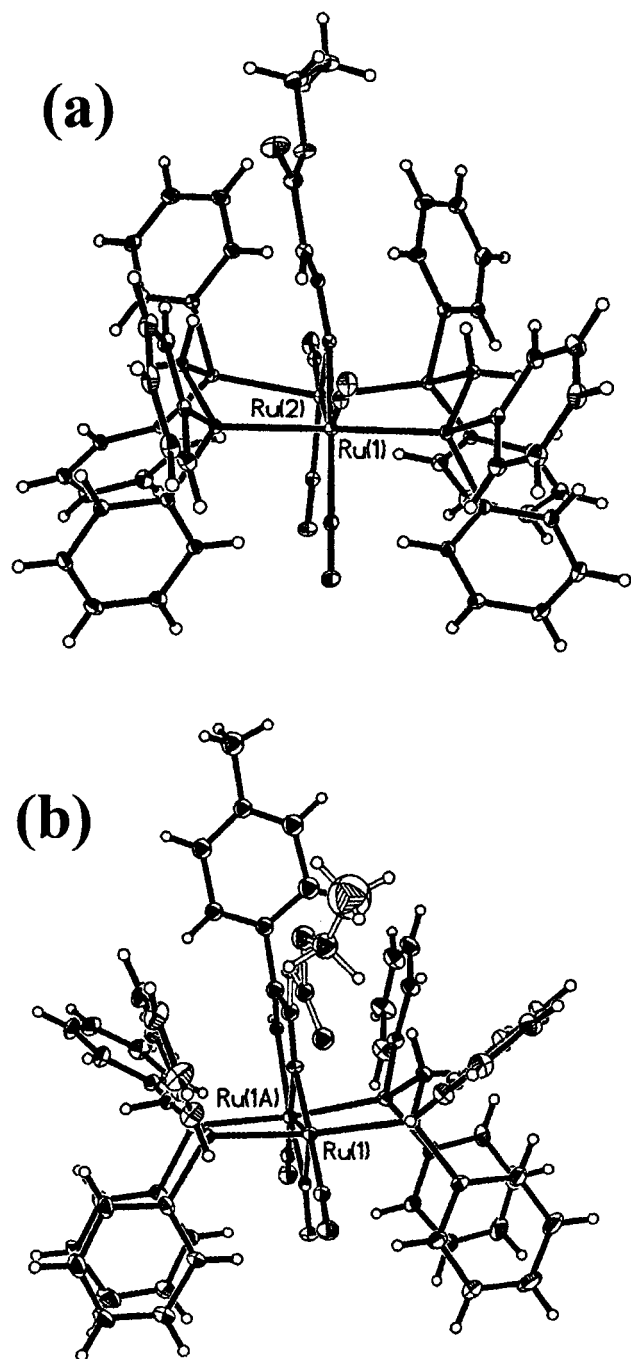
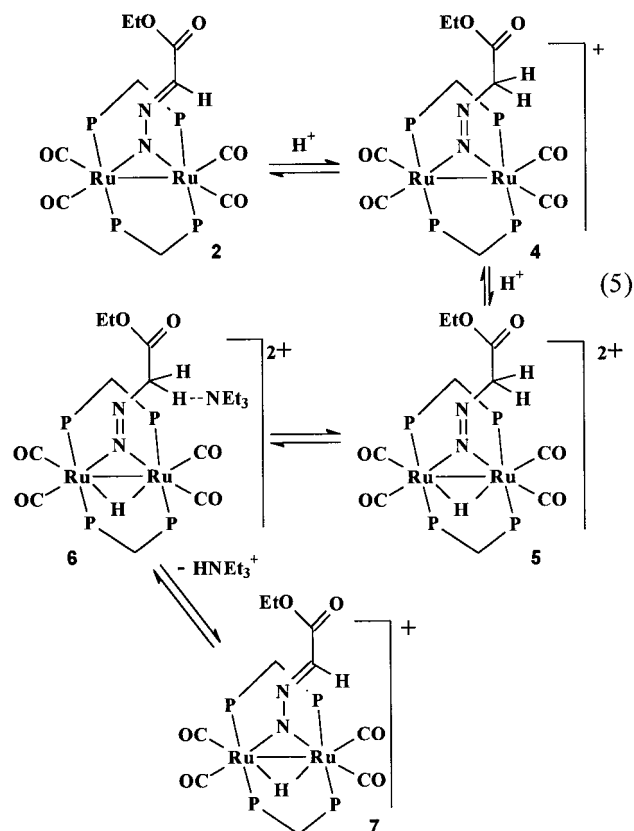


Figure 3. The different conformations of the diazo ligand in complexes **2** and **3b** that lead to large differences in chemical shifts of the ethoxy protons.

then, Ru should have an 18-electron configuration but RuA might have a 16-electron or 18-electron configuration. It may be convenient to consider the cycloaddition involving nucleophilic attack by the lone pair on N(2) in **2** (and electrophilic attack by ruthenium) on the alkyne as shown in Scheme 1. The stereochemistry of the product could then be understood in terms of the canonical forms **3A** (16-e at RuA) and **3B** (18-e at RuA). The representations **3A** and **3B** of Scheme 1 do not explicitly show conjugation in the diazoester unit, but this is likely to be similar to that for **2** (Chart 1), as indicated by similar values of $\nu(\text{C}=\text{O}) = 1627$ and 1632 cm^{-1} in **3b** and **2**, respectively.

The NMR spectra of **3b** are consistent with the solid-state structure. The $^{31}\text{P}\{\text{H}\}$ NMR spectrum displayed two multiplets at $\delta = 35.5$ and 33.5 for the phosphorus atoms of the dppm ligands. The ^1H NMR spectrum contained two multiplets at $\delta = 3.0$ and 2.5 for the CH_2P_2 protons of the dppm ligands and a singlet resonance at $\delta = 6.3$ due to $\text{CH}=\text{N}$ proton. The $\text{RuCH}=\text{C}$ proton resonance was not observed and is presumed to be obscured by the intense aryl resonances. The ethoxy resonances were observed at $\delta = 2.3$ (CH_2) and at $\delta = 0.6$ (CH_3) and are markedly different from those in complex **2** ($\delta = 4.2$ and 1.5 , respectively). The difference reflects the different conformations about the $\text{N}=\text{C}$ bond, and the ethyl protons of **3b** lie in a shielding zone between phenyl groups, as illustrated in Figure 3. The ethoxy group in **2** lies beyond this zone, and therefore normal chemical shifts are observed. There is greater steric hindrance in **3b** than in **2**, and **3b** does not exhibit the fluxionality due to rotation of the $\text{CO}_2\text{-Et}$ group that was shown to occur in **2**. The $^{13}\text{C}\{\text{H}\}$ NMR spectrum for a ^{13}C -labeled sample of **3b** displayed three carbonyl resonances, a multiplet at $\delta = 270$ for the bridging CO and multiplets at $\delta = 213.6$ and 208.5 for the two terminal carbonyls.

Protonation of Complex 2: Synthesis of $[\text{Ru}_2(\mu\text{-H})(\text{CO})_4\{\mu\text{-NNCH}_2\text{CO}_2\text{Et}\}(\mu\text{-dppm})_2][\text{BF}_4]_2$, $5[\text{BF}_4]_2$. The reaction of $\text{HBF}_4\cdot\text{Et}_2\text{O}$ with complex **2** in CD_2Cl_2 solution occurred according to eq 5. At -20°C , the



cationic complex **4** $[\text{BF}_4]$ was the major product, but at room temperature, further protonation occurred to give complex **5** $[\text{BF}_4]_2$. Complex **4** was identified only by its spectroscopic properties (see later), but complex **5** was isolated as the tetrafluoroborate salt and was fully characterized.

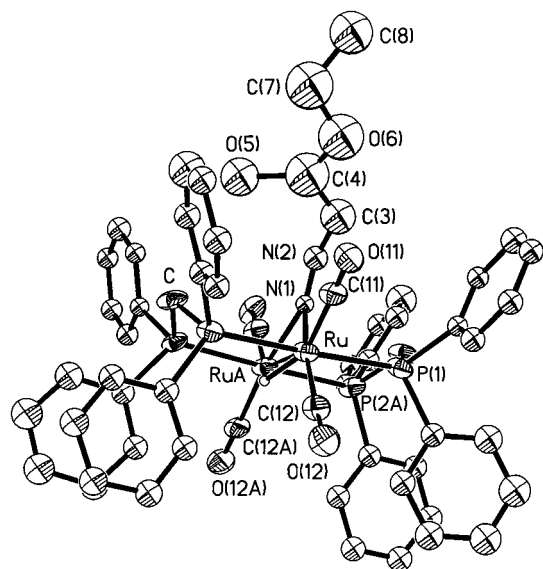


Figure 4. A view of the structure of the dicationic complex **5**. The hydride shown bridging the Ru–Ru bond was located but not refined. There is disorder in the diazo ligand and in two of the phenyl groups that is not shown (see text).

Table 3. Selected Bond Distances and Angles in 5

Bond Distances (Å)			
Ru–RuA	2.970(2)	Ru–P(1)	2.403(3)
Ru–P(2)	2.400(3)	Ru–C(11)	1.88(1)
Ru–C(12)	1.93(1)	Ru–N(1)	1.90(1)
RuA–N(1)	2.25(1)	N(1)–N(2)	1.21(2)
C(11)–O(11)	1.12(1)	C(12)–O(12)	1.16(1)
Bond Angles (deg)			
P(1)–Ru–N(1)	82.9(4)	P(2)–Ru–N(1)	96.0(4)
P(2)–Ru–P(1)	177.61(9)	Ru–N(1)–RuA	91.2(4)
N(2)–N(1)–Ru	139(1)	N(2)–N(1)–RuA	129(1)
C(11)–Ru–P(1)	89.0(3)	C(12)–Ru–P(2)	88.9(3)

The structure of the dication **5** is shown in Figure 4, and selected distances and angles are in Table 3. The structure solution was again complicated by disorder. A crystallographic C_2 axis passes through the center of the $Ru_2(\mu\text{-dppm})_2$ ring, and the N(1)N(2)CH₂CO₂Et atoms are disordered over equivalent positions by the 2-fold rotation. There is probably also further disorder of the ethoxy group which was not resolved. Hence the CH₂CO₂Et group is poorly defined.

Complex **5** contains a *trans,trans*- $Ru_2(\mu\text{-dppm})_2$ unit, in a boat conformation similar to that in **2** and **3**, and there are four terminal carbonyl ligands and the bridging N₂CH₂CO₂Et ligand. A hydride ligand bridges the Ru–RuA bond and was tentatively located but not refined [Figure 4, Ru–H = 1.6 Å, RuA–H = 1.7 Å, Ru–H–RuA = 125°]. The Ru–Ru distance [2.970(2) Å] is markedly longer than that in the parent complex **2** [2.8550(4) Å] but still suggests the presence of a weak RuRu single bond.^{6,7,9,13} Protonation of metal–metal bonds usually leads to a significant increase in M–M bond distance.¹³ Two BF₄[−] ions were identified for each diruthenium complex ion, thus confirming the dicationic nature of **5**. Although the atoms of the N₂CH₂CO₂Et

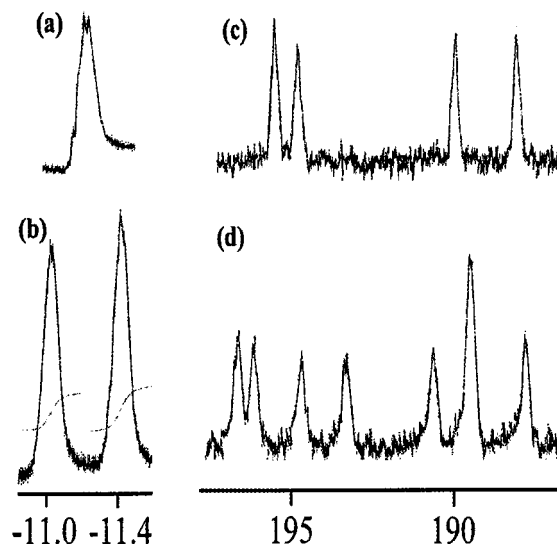


Figure 5. The variable temperature NMR spectra of complex **5**: (a and b) the hydride resonance in the ¹H NMR spectrum at room temperature and at −90 °C, respectively; (c and d) the carbonyl resonances in the ¹³C NMR spectrum at room temperature and at −90 °C, respectively. At low temperature, separate resonances for **5a** and **5b** (eq 6) are observed.

unit were not accurately defined, it is apparent from Figure 4 that the N₂CCO₂ atoms are no longer coplanar in **5** [the dihedral angle N(1)N(2)C(3)C(4) = −87°], as expected if conjugation is lost by protonation at carbon (eq 5). The lack of extended π -conjugation is also clear from the IR spectrum, which gives a normal value of $\nu(\text{CO}) = 1729 \text{ cm}^{-1}$ for the ester carbonyl group, a value much higher than in the conjugated complex **2**, [$\nu(\text{CO}) = 1632 \text{ cm}^{-1}$].

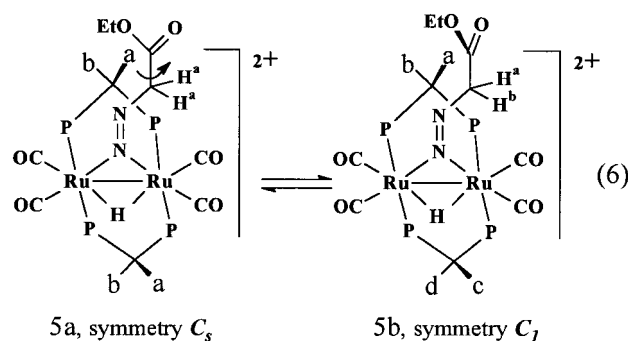
The structure of **5** was further defined by its NMR spectra. The ³¹P{¹H} NMR spectrum contained two overlapping signals at $\delta = 21.4$ and 21.1, and the ¹³C{¹H} NMR spectrum of a ¹³CO-enriched sample contained four peaks at $\delta = 195.8$, 195.0, 190.2 and 188.4, due to the four terminal carbonyls. The ¹H NMR spectrum contained the expected resonances for the CH₂P₂ protons of the dppm ligands [$\delta = 3.73$ and 3.40] and ethoxy protons [$\delta = 4.45$ (CH₂) and $\delta = 1.40$ (CH₃)], and the Ru₂(μ -H) group was indicated by a resonance at $\delta = -11.10$, which appeared as a quintet due to coupling ²J(PH). A sharp singlet at $\delta = 4.96$ was assigned to the NNCH₂ protons and confirmed by the observation of its correlation with the adjacent carbonyl carbon atom present at $\delta = 168$ in the ¹³C{¹H} NMR spectrum by a ¹H¹³C HMBC experiment and to the directly bound carbon at $\delta = 82.5$ by a ¹H¹³C HSQC experiment. Hence protonation of **2** at both the Ru–Ru bond and the NNCH atom is confirmed.

The IR spectrum of **5** displays four peaks at 2097, 2074, 2048, and 2030 cm^{−1} for the four terminal carbonyl ligands. In addition, there was a band assigned to $\nu(\text{N}=\text{N}) = 1548 \text{ cm}^{-1}$, in the accepted range for diazonium complexes.²

Complex **5** exhibited fluxional behavior in solution at room temperature, and this was frozen out below −60 °C. At −90 °C, two isomers were present in almost equal amounts, each displaying a hydride resonance signal in the ¹H NMR spectrum and four terminal carbonyl

(13) (a) Alcock, N. W.; Raspin, K. A. *J. Chem. Soc. A* **1968**, 2108. (b) Kauffmann, Th.; Beissner, G.; Koppelman, E.; Kuhlmann, D.; Schott, A.; Schrecken, H. *Angew. Chem., Int. Ed. Engl.* **1968**, 7, 131. (c) Johnson, K. A.; Gladfelter, W. L. *Organometallics* **1992**, 11, 2534. (d) Hursthouse, M. B.; Jones, R. A.; Abdul Malik, K. M.; Wilkinson, G. *J. Am. Chem. Soc.* **1979**, 101, 4129.

resonances in the $^{13}\text{C}\{\text{H}\}$ NMR spectrum (Figure 5). Interestingly, the two isomers have different symmetries. One isomer, **5a**, has apparent C_s symmetry. Thus, it gives a single CH_2O resonance in the ^1H NMR at $\delta = 4.30$ and two CH_2P_2 resonances at $\delta = 3.65$ and 2.70. The other isomer, **5b**, appears to have no symmetry (C_1). Thus, it gives two resonances due to diastereotopic $\text{CH}^a\text{H}^b\text{O}$ protons of the ethoxy group and two pairs of CH_2P_2 resonances at $\delta = 5.60, 3.65$ and 5.20, 3.85 with the assignments confirmed by the ^1H - ^1H correlated spectrum (COSY). This low symmetry form **5b** is likely to resemble the solid-state structure (Figure 4) in which the carboxyl group and $\text{N}(1)\text{N}(2)\text{C}(3)$ planes are roughly orthogonal and therefore there is no mirror plane. The more symmetrical isomer **5a** has effective C_s symmetry, and the conformation is probably similar to that in complex **2**. The rotation about the $\text{C}(3)$ - $\text{C}(4)$ bond needed to interconvert **5a** and **5b** (eq 6) is



presumably restricted due to steric effects, since $\text{C}(3)$ - $\text{C}(4)$ multiple bond character is not expected in **5**.

When complex **5** was dissolved in acetone- d_6 , slow exchange of the NCH_2 protons with deuterium from the solvent occurred. The resonance at $\delta = 4.96$ (NCH_2) decayed and a new isotopically shifted resonance at $\delta = 4.90$ (NCHD) grew; over long periods, both decayed as the NCD_2 group was formed. This shows that the protonation is reversible at the $\text{N}=\text{CH}$ center of **2** (eq 5). Reaction of complex **5** with the base triethylamine at -15°C gave a new complex, **6**, which was only partially characterized but which certainly maintained a $\text{Ru}_2(\mu\text{-H})$ group having $\delta = -8.9$. On warming, complex **6** formed an equilibrium with another complex, **7**, whose formation from **5** involves selective deprotonation at carbon (eq 5). Complex **7** is therefore an isomer of complex **4**. The diazo and diazonium isomers **4** and **7** are readily distinguished by their NMR properties, particularly by the absence or presence of a hydride resonance and of $\text{CH}=\text{N}$ or CH_2N resonances, respectively (Table 4). Complex **6** failed to give a resolved

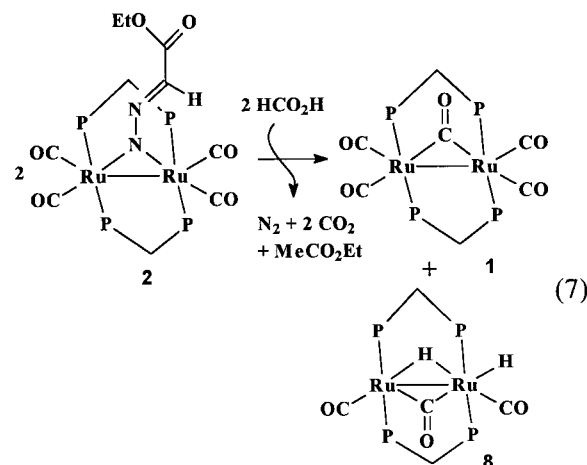
Table 4. Comparison of the NMR Properties of Complexes 2, 4, 5, 6, and 7

	2	4	5	6	7
$\delta(\text{CHN})$	5.8 ^a	4.5 ^b	4.96 ^b	<i>c</i>	5.9 ^a
$\delta(\text{CH}_2\text{O})$	4.3	4.2	4.45	4.20	4.4
$\delta(\text{CH}_3)$	1.5	1.2	1.40	1.38	1.5
$\delta(\text{CH}_2\text{P}_2)$	3.1, 3.1	3.6, 3.9	3.4, 3.7	2.7, 2.9	3.5, 3.7
$\delta(\text{RuH})$			-11.1	-8.9	-11.5
$\delta(\text{CHN})$	110 ^a	86 ^b	92.5 ^b	<i>c</i>	112 ^a
$\delta(\text{P})$	26.5, 32.4	26.6, 32.9	21.1, 21.4	30.7, 30.9	18.2, 23.6

^a $\text{CH}=\text{M}$ / CH_2N . ^c Not observed. The assignment of CHN resonances was confirmed by recording the ^1H - ^{13}C correlated spectrum (gHSQC).

resonance in the regions for either $\text{CH}=\text{N}$ or CH_2N groups. It is tentatively suggested that it may contain a $\text{HCH}\cdots\text{NET}_3$ hydrogen bond, leading to a very broad resonance. These data clearly confirm that protonation of **2** is kinetically controlled to give **4**, while deprotonation of **5** occurs at carbon to give **7**.

The Reactivity of Complex 2 to Formic Acid. At room temperature, the addition of an excess of formic acid to a solution of **2** in CD_2Cl_2 caused an immediate color change from brown-red to orange. After an induction period, the evolution of a gas, identified as a mixture of CO_2 and H_2 , was observed. Once started, the gas evolution was complete in a few minutes to leave a wine-red solution. No formic acid remained at this stage, and two known complexes **1** and $[\text{Ru}_2(\mu\text{-H})(\text{H})(\mu\text{-CO})(\text{CO})_2(\mu\text{-dppm})_2]$, **8**,¹⁴ were the only ruthenium complexes present, in about equal amounts, in the final solution. It is apparent from the above observations that catalytic decomposition of HCOOH to give $\text{CO}_2 + \text{H}_2$ occurred.¹⁴ The ethyl diazoacetate ligand in **2** was converted to ethyl acetate, which was identified by its NMR spectrum. Complex **8** is known to be an active catalyst for decomposition of formic acid in dichloromethane solution (complex **1** is also a catalyst but only in acetone solution), so the induction period is presumed to be associated with formation of complex **8**.¹⁴ The stoichiometric reaction can be described by eq 7. It is



likely that the ethyl acetate is formed by decomposition of transient $\text{EtO}_2\text{CCH}_2\text{NNH}$ with elimination of N_2 , by analogy to the known reaction of alkyldiazenes.¹⁵

The catalytic reaction proceeded much faster when carried out in acetone- d_6 , and the final ruthenium complexes were again **1** and **8**. However, ethyl acetate was formed in low yield and a second unidentified organic product was formed as the major product.

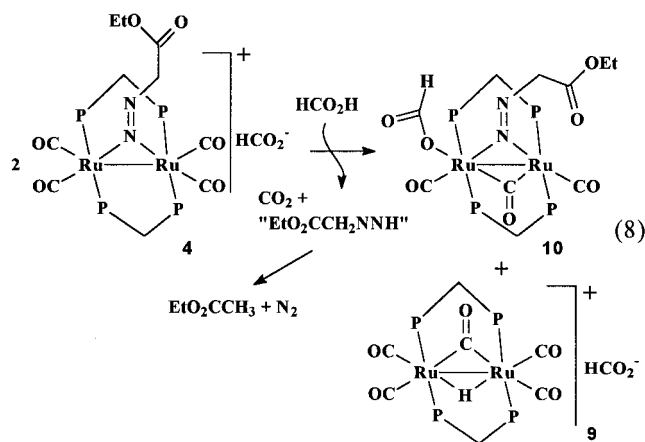
The reaction of formic acid with complex **2** was studied by a variable temperature NMR experiment in order to identify reaction intermediates. At a temper-

(14) (a) Gao, Y.; Kuncheria, J.; Jenkins, H. A.; Puddephatt, R. J.; Yap, G. P. A. *J. Chem. Soc., Dalton Trans.* **2000**, 3212. (b) Gao, Y.; Kuncheria, J.; Yap, G. P. A.; Puddephatt, R. J. *Chem. Commun.* **1998**, 2365.

(15) Ackermann, M. N.; Hallmark, M. R.; Hammond, S. K.; Roe, A. N. *Inorg. Chem.* **1972**, *11*, 3076. It is also possible that nitrogen loss occurs before the reductive elimination step. A GC-MS study of a reaction mixture after a reaction in acetone solution showed a compound present with $m/z = 116$, as expected for the diazene or its isomeric form $\text{EtO}_2\text{CCH}=\text{NNH}_2$, as well as at $m/z = 88$, for ethyl acetate.

ature below $-10\text{ }^{\circ}\text{C}$, only the complex cation $[\text{Ru}_2(\text{CO})_4(\mu\text{-NNCH}_2\text{CO}_2\text{Et})(\mu\text{-dppm})_2]^+$, **4**, as the formate salt, was observed in solution. Its spectroscopic properties are identical to those of **4**[BF₄] (eq 5). The $^{31}\text{P}\{\text{H}\}$ NMR spectrum of **4** displays two multiplets at $\delta = 32.9$ and 26.6 for the dppm phosphorus atoms. The ^1H NMR spectrum contained a singlet at $\delta = 4.5$ for the CH₂N protons, typical ethoxy resonances at $\delta = 4.2$ [q, CH₂] and $\delta = 1.2$ [t, CH₃], and two resonances for the CH₂P₂ protons at $\delta = 3.9$ and 3.6 . The $^{13}\text{C}\{\text{H}\}$ NMR spectrum of a sample prepared from ^{13}C -labeled **2** contained four resonances for terminal carbonyl ligands at $\delta = 210.9$, 210.8 , 194.6 , and 193.1 . The CH₂N resonance in the $^{13}\text{C}\{\text{H}\}$ NMR spectrum was found at $\delta = 86$. The NMR properties are similar to those of complex **5** described above but without the hydride resonance. Further protonation of **4** to give **5** was not observed in reactions with formic acid.

When the above solution was warmed to $6\text{ }^{\circ}\text{C}$, complex **4** decomposed to give a new complex, **10**, and then the known complex $[\text{Ru}_2(\mu\text{-H})(\mu\text{-CO})(\text{CO})_4(\mu\text{-dppm})_2]^+$, **9**.¹⁴ Complex **10** was transient; as it decayed, the concentration of **9** increased until the ratio of concentrations of **10**:**9** reached roughly 1:1, after which new products were observed. Complex **10** was characterized by its NMR spectra since it could not be isolated. The $^{31}\text{P}\{\text{H}\}$ NMR spectrum of **10** contained two multiplets at 25.8 and 24.4 , indicative of the symmetrical *trans* arrangement of the dppm ligands in **10**. The ^1H NMR spectrum displayed two multiplets at $\delta = 4.05$ and 3.60 for the methylene hydrogens of dppm ligands, a singlet at $\delta = 4.55$ for the CH₂N protons, and resonances for the ethoxy group at $\delta = 2.6$ [q, CH₂] and 0.6 [t, CH₃]. A new singlet resonance, attributed to coordinated formate, was present at $\delta = 9.4$. There is a marked difference in chemical shifts of the ethoxy resonances of **10** compared to those in **2** and **4** and the values are similar to those in **3**, suggesting a change in conformation of the diazonium ligand. Loss of a carbonyl is needed to allow this conformational change and to provide the fifth carbonyl present in the other product, complex **9**. The overall reaction to this point is then proposed to occur according to eq 8, bearing in mind that the structure of **10** is tentative.



Complex **10** is formed by displacement of a carbonyl ligand from **4** by formate, and it can then lose CO₂ from the formate to make a hydride that can reductively eliminate with the diazonium group to give the unstable

diazine "EtO₂CCH₂N=NH". This eliminates N₂ to give ethyl acetate in dichloromethane solution or reacts in more complex ways in acetone solution.¹⁵

When the solution was warmed to $20\text{ }^{\circ}\text{C}$, the catalysis began and concentrations of both **9** and **10** decreased. At the end of the reaction, the chief ruthenium products were complexes **1** and **8**. Complex **1** is formed simply by deprotonation of complex **9** as the concentration of formic acid decreases. Complex **8** is formed by decomposition of **10** under conditions with no free CO to convert the "Ru₂(CO)₃(μ-dppm)₂" to the pentacarbonyl derivative **1** or **9**. Reaction of "Ru₂(CO)₃(μ-dppm)₂" with formic acid can give CO₂ and complex **8**. Once coordinatively unsaturated complexes such as **8** are formed, the catalysis becomes very fast and is complete within minutes.¹⁴ The induction period for catalysis is associated with the preliminary chemistry.

Discussion

Complex **2** represents the first example of fully characterized diruthenium diazoalkane complex and the diazoalkane in **2** is shown to act as a 2-electron ligand. This bonding mode has not been structurally characterized previously in binuclear diazoalkane complexes,² and it is suggested that conjugation through the ester substituent gives added stability in complex **2**.

Complex **2** is electron-rich and has a number of possible sites for electrophilic attack, of which the lone pair on the angular β-nitrogen atom N(2), the methine carbon C(3), and the Ru–Ru bond can be considered prime candidates. In reactions with protons, the first reaction occurs rapidly at C(3) to give a diazonium complex and then, with the strong acid H[BF₄], slower attack occurs at the ruthenium–ruthenium bond to give a bridging hydride. With the weaker acid HCO₂H, only monoprotection at carbon occurs and then the formate coordinates with displacement of CO. Then decomposition by loss of CO₂ from formate, and formation of dinitrogen and ethyl acetate from the reduced diazoalkane, occurs.

In contrast to the site of proton attack, the reaction with the alkynes RCCH, R = phenyl or 4-tolyl, appear to involve nucleophilic attack by the lone pair on N(2). Mechanistically, it is likely that reaction is initiated by coordination of the alkyne to ruthenium, followed by nucleophilic attack by nitrogen leading to formation of a novel metallacycle in complexes **3**. Evidently the 2-electron bridging diazoalkane can display a diverse pattern of reactivity.

Experimental Section

All manipulations were carried out in an atmosphere of dry nitrogen, using either standard Schlenk techniques or a glovebox. Solvents were dried and distilled prior to use. The complex $[\text{Ru}_2(\mu\text{-CO})(\text{CO})_4(\mu\text{-dppm})_2]$ was synthesized according to the literature procedure.⁷ ^1H , ^{13}C , and ^{31}P NMR spectra were recorded using a Varian Inova 600 or 400 or Gemini 300 spectrometer. Mass (and GC-MS) spectra were recorded using a Finnigan Mat 8200 spectrometer.

Synthesis of $[\text{Ru}_2\{\mu\text{-NNCHCO}_2\text{Et}\}(\text{CO})_4(\mu\text{-dppm})_2]$, **2.** Ethyl diazoacetate (37 μL, 0.32 mmol) was added to a solution of $[\text{Ru}_2(\mu\text{-CO})(\text{CO})_4(\mu\text{-dppm})_2]$, **1**, (0.27 g, 0.253 mmol) in CH₂-Cl₂ (20 mL). The solution color changed from orange-yellow to red in 20 min. The volume of solution was reduced to 2 mL

Table 5. Crystal Data and Structure Refinement for Complexes 2, 3a, 3b, and 5

	2	3a.0.5CH₂Cl₂	3b	5
formula	C ₆₂ H ₅₄ N ₂ O ₅ P ₄ Ru ₂	C _{65.5} H ₅₀ ClN ₂ O ₅ P ₄ Ru ₂	C ₆₆ H ₅₇ N ₂ O ₅ P ₄ Ru ₂	C ₅₉ H ₄₆ B ₂ Cl ₂ F ₈ N ₂ O ₆ P ₄ Ru ₂
fw	1233.09	1306.55	1284.16	1449.52
cryst sys	monoclinic	tetragonal	tetragonal	tetragonal
space group	<i>P</i> 2(1)/ <i>n</i>	<i>P</i> 4(1)2(1)2	<i>P</i> 4(3)2(1)2	<i>P</i> 4(2)2(1)2
<i>a</i> /Å	11.9163(6)	15.293(1)	15.1244(6)	18.5555(4)
<i>b</i> /Å	22.118(1)	15.293(1)	15.1244(6)	18.5555(4)
<i>c</i> /Å	22.351(1)	27.764(2)	28.2910(15)	20.0822(4)
β /deg	98.903(1)	90	90	90
<i>V</i> /Å ³	5820.1(5)	6493.2(9)	6471.5(5)	6914.4(3)
<i>Z</i>	4	4	4	4
<i>d</i> (calcd)/Mg m ⁻³	1.407	1.337	1.318	1.392
<i>TK</i>	213(2)	200(2)	223(2)	150(2)
λ /Å	0.710 73	0.710 73	0.710 73	0.710 73
abs coeff/mm ⁻¹	0.678	0.652	0.613	0.674
abs corr	integration	integration	integration	integration
reflins	33 304	38 214	32 919	33 093
GOF	1.086	0.927	1.106	1.064
R1, wR2 (<i>I</i> > 2 σ (<i>I</i>))	0.047, 0.133	0.078, 0.160	0.058, 0.149	0.082, 0.225

by vacuum, and pentane (80 mL) was then added to precipitate the brown-yellow product, which was filtered off, washed with pentane, and then dried under vacuum. Yield: 56%. Anal. Calcd for C₅₈H₅₀N₂O₆P₄Ru₂: C, 58.2; H, 4.2; N, 2.3. Found: C, 58.1; H, 4.2; N, 1.85. IR (cm⁻¹, Nujol): ν (CO) = 1974, 1955, 1929, and 1900; ν (C=O) = 1632; ν (C=N) = 1574. NMR in CD₂-Cl₂ at 20 °C: δ (³¹P) = 26.5 [br m, dppm]; 32.4 [br m, dppm]; δ (¹H) = 5.8 [br s, 1H, CHCO(O)Et]; 3.1 [br m, 4H, P-CH^aH^b-P]; 4.3 [br m, 2H, -CH₂CH₃]; 1.5 [br s, 3H, -CH₂CH₃]; δ (¹³C) = 214.8, 210, 198.4, 198 [br m, terminal CO]; 167.0 [br s, -C(O)-OEt]; 110.0 [br s, CHCO(O)Et]; 59.0 [s, -CH₂CH₃]; 30.0 [br s, P-CH₂-P]; 18.0 [s, -CH₂CH₃]. NMR in CD₂Cl₂ at -40 °C: isomer **2a** δ (³¹P) = 32.0 [br m, dppm]; 26.0 [br m, dppm]; 5.65 [br s, 1H, CHCO(O)Et]; 4.25 [br s, 2H, -CH₂CH₃]; 1.55 [br s, 3H, -CH₂CH₃]; isomer **2b** δ (³¹P) = 32.0 [br m, dppm]; 25.8 [br m, dppm]; δ (¹H) = 5.80 [br s, 1H, CHCO(O)Et]; 4.15 [br s, 2H, -CH₂CH₃]; 1.32 [br s, 3H, -CH₂CH₃]. Resonances for the CH₂P₂ protons were not fully resolved, with three broad resonances at δ = 3.05, 2.9, 2.7 observed. The ratio **2a:2b** = 3:2.

The Reaction of 2 with CO. A stream of CO was bubbled through a solution of **2** (15 mg, 0.013 mmol) in CD₂Cl₂ (0.6 mL) in a rubber septum-sealed NMR tube for 15 min. The NMR tube was then sealed. After 24 h, only traces of complex **2** remained and complex **1** was formed and identified by its ¹H and ³¹P NMR spectra.

Synthesis of [Ru₂(μ -CO)(CO)₂(μ -NN(CHCO₂Et)(CRCH))-(μ -dppm)₂], **3a, R = Ph.** PhC≡CH (15 μ L, 0.14 mmol) was added to a stirred solution of **2** (0.1 g, 0.08 mmol) in CH₂Cl₂ (20 mL). After 3 h the volume was reduced under vacuum to 2 mL and pentane (60 mL) was added to precipitate the brown-yellow product, which was filtered off, washed with pentane, and dried under vacuum. Yield: 66%. Anal. Calcd for **3a**·1/2CH₂Cl₂, C_{65.5}H₅₇ClN₂O₅P₄Ru₂: C, 59.9; H, 4.4; N, 2.1. Found: C, 59.4; H, 4.4; N, 1.9. IR (cm⁻¹, Nujol): ν (CO) = 1893, 1869, 1661; ν (C=O of the diazoalkane) = 1627. NMR in CD₂-Cl₂ at 20 °C: δ (³¹P) = 35.5 [m, dppm]; 33.5 [m, dppm]; δ (¹H) = 6.3 [s, 1H, CHCO(O)Et]; 3.0 [m, 2H, P-CH^aH^b-P]; 2.5 [m, 2H, P-CH^aH^b-P]; 2.3 [q, 2H, -CH₂CH₃]; 0.5 [t, 3H, -CH₂CH₃]. For a sample of ¹³CO-labeled **3**: δ (¹³C) = 277 [m, bridging CO], 213.6, 208.5 [m, terminal CO]. Complex **3b**, R = 4-MeC₆H₄, was synthesized similarly. Yield: 62%. Anal. Calcd for **3b**·1.5CH₂Cl₂, C_{67.5}H₆₁Cl₃N₂O₅P₄Ru₂: C, 57.4; H, 4.35; N, 2.0. Found: C, 57.6; H, 3.6; N, 1.3. NMR in CD₂Cl₂ at 20 °C: δ (³¹P) = 35.4 [m, dppm]; 33.8 [m, dppm]; δ (¹H) = 6.3 [s, 1H, CHCO₂Et]; 3.0 [m, 2H, P-CH^aH^b-P]; 2.5 [m, 2H, P-CH^aH^b-P]; 2.25 [q, 2H, -CH₂CH₃]; 0.5 [t, 3H, -CH₂CH₃].

Synthesis of [Ru₂(μ -H)(CO)₄(μ -NNCH₂CO₂Et)(μ -dppm)₂]-[BF₄]₂, **5[BF₄]₂.** To a solution of **2** (35 mg, 0.03 mmol) in CD₂-Cl₂ (0.5 mL) in a septum-sealed NMR tube was added HBF₄·Et₂O (10 μ L, 0.07 mmol) by using a microsyringe. The solution

color changed immediately to red and then to brown-yellow in a few minutes. To this solution was layered 2 mL of ether carefully. Cubic yellow crystals suitable for X-ray diffraction studies were obtained in 48 h. The crystals were washed with pentane and dried under vacuum. Yield: 20 mg (48%). Anal. Calcd for C₅₈H₅₂B₂F₈N₂O₆P₄Ru₂: C, 50.7; H, 3.8; N, 2.0. Found: C, 50.1; H, 3.9; N, 1.7. The borderline analysis is due to the fractional presence of dichloromethane. IR (Nujol, cm⁻¹): ν (CO) = 2097, 2074, 2048, 2030; ν (C=O of diazoalkane) = 1729, ν (N=N) = 1548. NMR in CD₂Cl₂ at 20 °C: δ (³¹P) = 21.4 [m, dppm], 21.1 [m, dppm]; δ (¹H) = 4.96 [s, 2 H, -CH₂NN]; 3.73 [br m, 2H, P-CH^aH^b-P]; 3.40 [br m, 2H, P-CH^aH^b-P]; 4.45 [q, 2H, ³J_{H-H} = 7 Hz, -CH₂CH₃]; 1.40 [t, 3H, ³J_{H-H} = 7 Hz, -CH₂CH₃]; -11.10 [quin, 1H, ²J_{P-H} = 10 Hz, μ -H]. For a sample of ¹³CO-labeled **5**, δ (¹³C) = 195.8, 195.0, 190.2, 188.4 [br s, terminal CO]. NMR in CD₂Cl₂ at -90 °C: resonances for **5a** and **5b** overlapped at δ (¹H) = ca. 5 [v br, NCH₂] and at δ (³¹P) = 21.2 [br m, dppm], 21.8 [br m, dppm]. **5a**: δ (¹H) = 3.65, 2.70 [m, each 2H, CH^aH^bP₂]; 4.30 [q, 2H, CH₂O]; 1.20 [t, 3H, CH₃]. **5b**: δ (¹H) = 5.60, 3.65; 5.20, 3.85 [m, each 1H, CH₂P₂]; 4.60, 4.45 [m, each 1H, CH₂O]; 1.20 [t, 3H, CH₃]. Resonances at δ (¹H) = -11.4 and -11.1 [br m, 1H, μ -H]; δ (¹³C) = 197, 196.5, 195, 193.6, 190.8, 189.6, 189.6, 189.6, 187.9 [br m, terminal CO] could not be assigned to a specific isomer.

Studies of the Reaction of 2 with HCOOH. (a) Room-Temperature Studies. To a solution of **2** (10 mg, 0.009 mmol) in CD₂Cl₂ (0.5 mL) in a septum-sealed NMR tube was added HCOOH (3 μ L, 0.06 mmol). The color of the solution changed immediately from brown-red to brown. After 3 h, gas bubbling was observed and the solution color changed to wine-red. The known complexes **1** and **8** were identified by their ¹H and ³¹P NMR spectra, and ethyl acetate was identified by its ¹H and ¹³C NMR spectra. Formic acid was absent at this stage.

The decomposition of formic acid was complete within 1 h when a similar reaction was carried out using acetone as the solvent. The major organic product was not fully characterized. NMR in acetone-*d*₆ at 20 °C: δ (¹H) = 4.32 [s]; 4.0 [q, ³J_{H-H} = 7 Hz]; 1.1 [t, ³J_{H-H} = 7 Hz]. δ (¹³C) = 152.5, 59.4, 11.8. GC-MS (*M*⁺): *m/z* = 116. A sample of EtO₂CCH=NNH₂ was synthesized according to a literature method for comparison.¹⁶ NMR in CD₂Cl₂ at 20 °C: *cis*-isomer: δ (¹H) = 1.20 [t, ³J_{H-H} = 7 Hz, 3H, CH₃CH₂-]; 4.20 [q, ³J_{H-H} = 7 Hz, 2H, CH₃CH₂-]; 6.42 [s, 1H, -CH₂NNH₂]; 6.85 [br s, -CH₂NNH₂]; δ (¹³C) = 14.0 [s, CH₃-CH₂-]; 59.8 [s, CH₃CH₂-]; 120.0 [s, -CH₂NNH₂]; 163.0 [s, CH₃-CH₂OOC(O)-]. *trans*-isomer: δ (¹H) = 1.20 [t, ³J_{H-H} = 7 Hz, 3H, CH₃CH₂-]; 4.2 [q, ³J_{H-H} = 7 Hz, 2H, CH₃CH₂-]; 7.0 [s, 1H,

(16) Staudinger, H.; Hammet, L.; Siegwart, J. *Helv. Chim. Acta* **1921**, *4*, 228.

-CHNNH₂]; 7.05 [br s, -CHNNH₂]; $\delta(^{13}\text{C}) = 23.0$ [s, CH₃CH₂-]; 60.8 [s, CH₃CH₂-]; 128.0 [s, -CHNNH₂]; 169.0 [s, CH₃CH₂O C(O)-].

(b) Low-Temperature Studies. A solution in CD₂Cl₂ was prepared as above but at -10 °C, and intermediates were identified by their NMR spectra as follows. [Ru₂(CO)₄(μ -NNCH₂CO₂Et)(μ -dppm)₂][HCOO], **4**[HCOO], was the only complex observed at -10 °C. NMR in CD₂Cl₂: $\delta(^{31}\text{P}) = 32.9$ [m, dppm], 26.6 [m, dppm]; $\delta(^1\text{H}) = 8.1$ [s, 1H, HCOO]; 4.5 [s, 2H, -CH₂NN]; 4.2 [q, 2H, ³J_{H-H} = 7.3 Hz, -CH₂CH₃]; 3.9 [m, 2H, P-CHP]; 3.6 [m, 2H, P-CHP]; 1.2 [t, 3H, ³J_{H-H} = 7.32 Hz]. For a sample prepared from the reaction of HCOOH with ¹³CO-labeled **2**: $\delta(^{13}\text{C}) = 210.9, 210.8, 194.6, 193.1$ [m, terminal CO]. At 6 °C, the known complex [Ru₂(μ -H)(μ -CO)(CO)₄(μ -dppm)₂][HCOO], **7**[HCOO], was observed as a minor product and identified by its NMR spectra.¹⁴ The major, but transient, product was tentatively identified as complex **10** (ratio **10:9** = 3:1). NMR in CD₂Cl₂ at 6 °C: $\delta(^{31}\text{P}) = 25.8$ [br m, dppm], 24.4 [br m, dppm]; $\delta(^1\text{H}) = 4.05$ [m, 2H, P-CHP]; 3.6 [m, 2H, P-CHP]; 2.6 [q, J_{H-H} = 7 Hz, 2H, -CH₂CH₃]; 0.6 [t, J_{H-H} = 7 Hz, 3H, -CH₂CH₃]. When the solution was warmed to 20 °C, both complexes **10** and **9** disappeared in 20 min. Complexes [Ru₂(μ -H)(H)(μ -CO)(CO)₂(μ -dppm)₂], **8**, and [Ru₂(μ -CO)(CO)₄(μ -dppm)₂], **1**, were observed in solution and free formic acid was absent.

X-ray Structure Determinations. Crystals of **2** were grown by slow evaporation of a saturated solution in toluene.

Crystals of **3a**, **3b**, or **5** were grown by diffusion of pentane (**3a**, **3b**) or ether (**5**) into a solution of the complex in CH₂Cl₂. Crystal data and refinement parameters are listed in Table 5. Data for **2**, **3a**, and **5** were collected using a Nonius Kappa-CCD diffractometer using COLLECT (Nonius, 1998) software. The unit cell parameters were calculated and refined from the full data set. Crystal cell refinement and data reduction was carried out using the Nonius DENZO package. The data were scaled using SCALEPACK (Nonius, 1998). Data for **3b** were collected by using a Siemens P4 diffractometer with XSCANS software. Refinement was carried out as above. The disordered C and O atoms in **3a**, **3b**, and **5** were treated isotropically while all other heavy atoms were anisotropic. For **3a**, **3b**, and **5** the correct choice of absolute structure was confirmed by refinement of the absolute structure factor (BASF = 0.00 in each case).

Acknowledgment. We thank the NSERC (Canada) for financial support.

Supporting Information Available: Tables of X-ray data in cif format. This material is available free of charge via the Internet at <http://pubs.acs.org>.

OM0102293